

Near-Infinite-Chain Polymers with Ge=Ge Double Bonds

Anna-Lena Thömmes,* Thomas Büttner, Bernd Morgenstern, Oliver Janka, Guido Kickelbick, Bart-Jan Niebuur, Tobias Kraus, Markus Gallei, and David Scheschkewitz*

In memory of Ian Manners

Abstract: Despite considerable interest in heteroatom-containing conjugated polymers, there are only few examples with heavier p-block elements in the conjugation path. The recently reported heavier acyclic diene metathesis (HADMET) allowed for the synthesis of a polymer containing Ge=Ge double bonds—albeit insoluble and with limited degree of polymerization. By incorporation of long alkyl chains, we now obtained soluble representatives, which exhibit degrees of polymerization near infinity according to diffusion-ordered NMR spectroscopy (DOSY) and dynamic light scattering (DLS). UV/Vis and NMR data confirm the presence of σ,π -conjugation across the silylene-phenylene linkers between the Ge=Ge double bonds. Favorable intermolecular dispersion interactions lead to ladder-like cylindrical assemblies as confirmed by X-ray diffraction (XRD), small angle X-ray scattering (SAXS) and DLS. AFM and TEM images of deposited thin films reveal lamellar ordering of extended polymer bundles.

Introduction

Polymers exhibit considerable advantages compared to many other materials such as high flexibility, light weight, low cost, low toxicity, and facile processability and handling. They are used in various applications, e.g. food conservation, clothes, furniture, encapsulation, membranes, medical implants, and many more.^[1] Conjugated polymers are extensively applied in commercial electronic devices^[2] and some even outperform silicon and germanium as semiconductors.^[3] Bulk conducting polymers can be tuned by alteration of the chemical composition: the incorporation of heteroelements, for instance, is essential to the *indirect* alteration of the band gap through secondary effects without incorporation into the conjugation path. As a technology-critical semiconductor,^[4] germanium is frequently employed in this context.^[5]

The availability of a variety of stable unsaturated compounds of the heavier p-block elements^[6] inspired new avenues in the design of conjugated systems. The heavy analogues of alkenes exhibit distinct properties due to differences in the topological and electronic structures: the Ge=Ge double bond motif, in stark contrast to the colorless alkenes, absorbs in the visible range in line with the inherently small HOMO–LUMO gap. The entire range of the visible spectrum can be addressed by changing the substituents: while most aryl and alkyl substituted digermenes are bright yellow,^[7] variable red-shifts can be achieved by B, Si, Ge and P substitution of the Ge=Ge bond^[8–11] or its incorporation into cyclic motifs.^[7i,12] Heavier alkenes with residual functionality allow for the incorporation of unsaturated bonding motifs into extended systems.^[13] In particular, the nucleophilic heavier analogues of vinyl anions^[8,9,14,15] have paved the way for the synthesis of arylene-bridged group 14 oligomers with element-element or element-carbon double bonds in the conjugation path.^[10,14,16–20]

Unsaturated motifs of heavier p-block elements in the repeat unit of conjugated polymers exert a *direct* influence on the band gap, but only a handful of such compounds are known^[2i] due to the inherent preparative challenges associated to heavier main group multiple bonding:^[6] typically, meticulous exclusion of air and water is a must to prevent the otherwise facile hydrolysis of the unsaturated motif. Bulky substituents are also required to kinetically stabilize the compounds against secondary intermolecular reactions.

[*] A.-L. Thömmes, T. Büttner, Prof. Dr. D. Scheschkewitz

Krupp-Chair for General and Inorganic Chemistry
Saarland University
66123 Saarbrücken, Germany
E-mail: anna-lena.thoemmes@uni-saarland.de
scheschkewitz@mx.uni-saarland.de

Dr. B. Morgenstern, Dr. O. Janka, Prof. Dr. G. Kickelbick
Inorganic Solid-State Chemistry
Saarland University
66123 Saarbrücken, Germany

Dr. B.-J. Niebuur, Prof. Dr. T. Kraus
INM—Leibniz-Institute for New Materials
66123 Saarbrücken, Germany

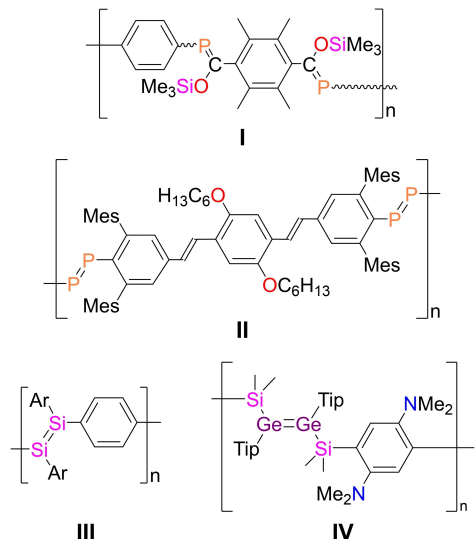
Prof. Dr. T. Kraus
Colloid and Interface Chemistry
Saarland University
66123 Saarbrücken, Germany

Prof. Dr. M. Gallei
Polymer Chemistry
Saarland University
66123 Saarbrücken, Germany

© 2024 The Author(s). Angewandte Chemie International Edition published by Wiley-VCH GmbH. This is an open access article under the terms of the Creative Commons Attribution Non-Commercial NoDerivs License, which permits use and distribution in any medium, provided the original work is properly cited, the use is non-commercial and no modifications or adaptations are made.

Pioneering work by the groups of Gates and Protasiewicz on poly(phosphaalkene)s such as **I** with P=C bonds in the conjugation path and polymerization degrees of $X_n=4.5$ to 21^[22] was soon complemented by the isolation of a poly(diphosphene) **II** with P=P bonds and $X_n=5.8$ (Scheme 1).^[23] In contrast, the only examples in case of group 14 had been the short oligo(disilene)s **III** ($X_n=2$ to 3)^[17] until our recent report on the heavier acyclic diene

metathesis (HADMET) of a phenylene bridged bis(digermene). The HADMET process results in polymer **IV** with Ge=Ge repeat units in the pathway of a σ,π -conjugated system.^[10] Although the degree of polymerization X_n of **IV** between 21 and 31 (depending on the method) is competitive with the P=C and P=P containing materials, its insolubility in all common organic solvents prevented a comprehensive analysis and—even more importantly—was assumed to be the limiting factor during chain growth. We now report on the synthesis of modified heavier acyclic dienes with solubility-increasing alkyl chains at silicon or nitrogen. Their polymerization by the HADMET procedure yields soluble rod-like polymers with essentially unlimited chain lengths. The increased solubility enables the full characterization of these Ge=Ge containing σ,π -conjugated polymers and their deposition as thin films with noteworthy patterns of lamellar bundles.



Scheme 1. Reported polymers containing heavier p-block multiple bonds: bridged poly(phosphaalkene) **I**,^[22] poly(diphosphene) **II** (Mes=2,4,6-trimethylphenyl),^[23] disilene oligomers **III**^[17] (Ar=1,1,3,3,5,5,7,7-octaethyl-s-hydridacen-4-yl) and poly(digermene) **IV** (Tip=2,4,6-triisopropylphenyl).^[10]

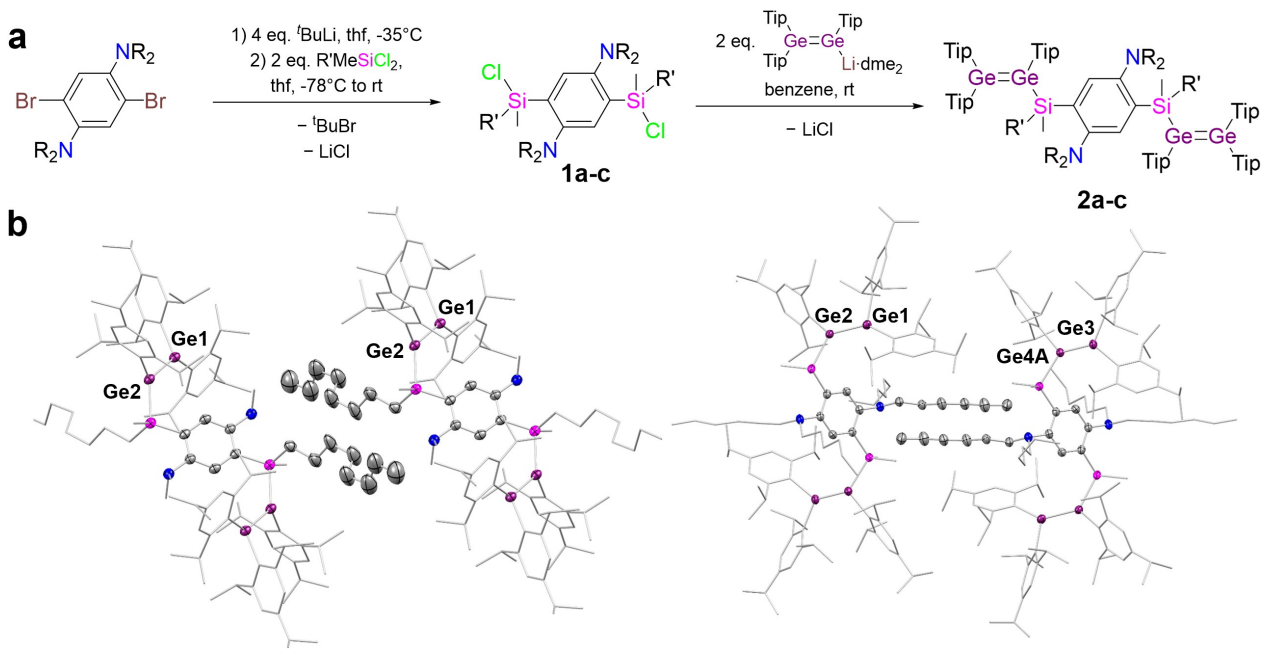


Figure 1. a) Synthesis of bis(chlorosilyl) linkers **1a–c** and substitution reactions with a lithium digermenide to bis(digermene)s **2a–c** (**1a,2a**: R=Me, R'=Oct, **1b,2b**: R=Hex, R'=Me, **1c,2c**:^[10] R=R'=Me). b) Adjacent molecules in the single crystal X-ray structures of bis(digermene) monomers **2a** (left) and **2b** (right).

centers at the silicon atoms. X-ray analysis of a colorless crystal reveals the structure of the *meso*-form (for details see Supporting Information).

For adaption of the amino groups, hexyl chains were attached to the nitrogen atoms in an earlier step of the linker synthesis (see Supporting Information). The achiral bis(chlorosilyl) linker **1b** with dihexylamino groups was obtained by reaction of the dilithiated precursor with Me_2SiCl_2 as colorless crystals in 75 % yield (Figure 1a).

Both, **1a** and **1b**, proved indeed suitable for twofold incorporation of the $\text{Ge}=\text{Ge}$ moiety by treatment with lithium digermenide $\text{Tip}_2\text{Ge}=\text{GeTip}(\text{Li}\cdot\text{dme}_2)$ affording bis(digermene)s **2a,b** as yellow crystals in isolated yields of 48 % and 61 %, respectively (Figure 1a). The increased steric demand in **2a,b** compared to *Si,Si,N,N*-tetramethyl substituted **2c**^[10] requires longer reaction times of 48 h. The incorporation of two longer alkyl chains at silicon completely suppresses the formation of the bis(digermene).

In the synthesis of bis(digermene) **2a**, the diastereomeric ratio of the precursor **1a** is retained in the reaction mixture ($\text{dr}=1:1$). In crystallized samples of **2a**, however, the *meso*-isomer is enriched to a ratio of $\text{dr}=1:7$ as determined by the intensity of the ^{29}Si NMR signals at 7.28 (rac) and 7.12 ppm (meso). The ^1H and ^{13}C NMR spectra of the two bis(digermene)s show similar shifts as those of previously reported silyl-substituted aryl digermenes.^[8,10,11d] ^1H NMR spectroscopy reveals characteristically downfield shifted singlets due to the protons at the phenylene linker each at 8.28 (**2a**) and 8.36 ppm (**2b**).

X-ray diffraction on single crystals obtained from saturated solutions (**2a**: hexane, RT; **2b**: Et_2O , -23°C) confirm the molecular structures of **2a** and **2b** in the solid state (Figures 1b and S30, S31 in Supporting Information). The $\text{Ge}=\text{Ge}$ distances of $2.2923(5)\text{ \AA}$ (**2a**) and $2.2742(5)/2.2972(9)\text{ \AA}$ (**2b**) are slightly shorter than the $\text{Ge}=\text{Ge}$ double bond lengths in the *Si,Si,N,N*-tetramethyl derivative **2c** (2.3038 \AA),^[10] and in asymmetrically substituted $\text{Tip}_2\text{Ge}=\text{GeTip}(\text{SiPh}_3)$ (2.3279 \AA),^[11d] but fit quite well the corresponding distances in tetrakis(trialkylsilyl)substituted digermenes ($2.266\text{--}2.298\text{ \AA}$).^[11a] The substituents at the double bonds are more or less *trans*-bent and twisted as common for digermenes, a manifestation of the shallow bending potential at the heavier double bonds.^[6b,24] The values for the *trans*-bent angle θ vary between $15.7(1)^\circ$ and $35.5(1)^\circ$, for the twisting angle τ between $17.9(1)^\circ$ and $21.8(1)^\circ$.

UV/Vis spectra of both bis(digermene) monomers **2a,b** exhibit the longest wavelength absorption at 431 nm, in the range of $\pi\rightarrow\pi^*$ transitions of the $\text{Ge}=\text{Ge}$ double bonds in aryl and silyl digermenes (406 to 438 nm),^[7a,c,8,10,11a,d,25] hence confirming the integrity of the double bond in solution. The high extinction coefficients of $\epsilon=27800$ (**2a**) and $33400\text{ L mol}^{-1}\text{ cm}^{-1}$ (**2b**) are in line with the large absorption cross sections typical of conjugated systems, notably also in hyperconjugated silyl-substituted systems.^[26,27] The presence of σ,π -conjugation in **2a,b** is confirmed by DFT calculations at the BP86-D3(BJ)/def2-SVP level of theory (Figure 2): the π -orbitals of the $\text{Ge}=\text{Ge}$ double bonds are represented by in-phase and out-of-phase combinations of both $\text{Ge}-\text{Ge}$

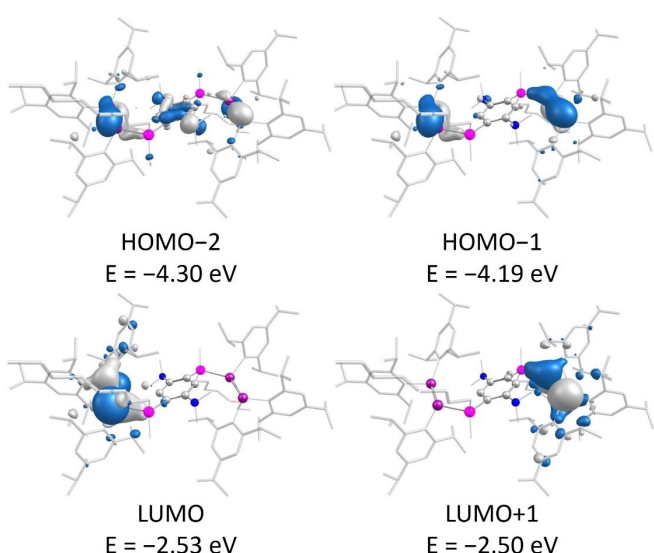
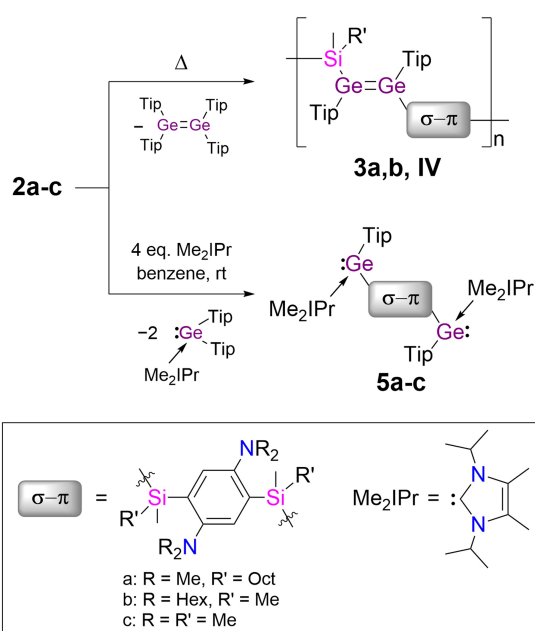


Figure 2. Selected frontier orbitals of bis(digermene) monomer **2a** (contour value 0.036). Hydrogen atoms omitted for clarity.

bonds, with visible mutual σ^* -contributions, separated by as much as 0.11 eV (**2a**) and 0.13 eV (**2b**). The corresponding unoccupied π^* -orbitals are equally non-degenerate, albeit with smaller separations of 0.03 and 0.08 eV, respectively. The LUMO + 2, located mainly at the aniline linker, exhibit contributions from the σ^* -orbitals at the silicon atoms in the conjugation path as well (see Supporting Information).

With these bridged digermenes as monomers in hand, we attempted the HADMET polymerization to the corresponding $\text{Ge}=\text{Ge}$ -containing polymers (Scheme 2). Heating of **2a,b** in solution led to the elimination of $\text{Tip}_2\text{Ge}=\text{GeTip}_2$ according to ^1H NMR monitoring. The appearance of broad signals in the ^1H , ^{13}C and ^{29}Si NMR spectra suggested the formation of the targeted polymers and the sharp signals of the molecular starting materials decrease in intensity. Polymerization of octyl-substituted monomer **2a** is observed at 65°C in benzene just as it had been in the case of the previously reported *Si,Si,N,N*-tetramethyl derivative **2c**.^[10] The hexylamino derivative **2b** requires heating to 105°C in toluene despite the sterically less demanding environment of the $\text{Ge}=\text{Ge}$ units. The additional stabilization is most likely due to favorable dispersion interactions between the Tip groups and the alkyl chains, which are increased in the presence of four instead of two long alkyl chains.^[28]

For a first estimation of the degree of polymerization X_n , the progress of the step-growth polymerization was monitored by integration of a characteristic ^1H NMR signal of the concomitantly formed by-product $\text{Tip}_2\text{Ge}=\text{GeTip}_2$.^[10] According to Carother's $X_n=(1-p)^{-1}$ correlation between the number-average degree of polymerization X_n and the conversion p of a bifunctional monomer in a condensation polymerization, $X_n=25$ for $p=96\%$.^[29] This is achieved after 44 h in the case of the previously reported *Si,Si,N,N*-tetramethyl substituted derivative **IV** whose further polymerization is prevented by its low solubility.^[10]



Scheme 2. HADMET polymerization of bis(digermene) monomers **2a–c** yielding soluble poly(digermene)s **3a,b** and previously reported insoluble **IV** and reaction of bis(digermene) monomers **2a–c** with *N*-heterocyclic carbene 1,3-diisopropylimidazol-4,5-dimethyl-2-ylidene (Me₂IPr) providing NHC-bis(germylene) adducts **5a–c** and Tip₂Ge–NHC.

As expected, the alkylated derivatives indeed exhibit a much higher solubility (vide infra) so that long polymer chains still remain available for further step-growth. In these cases, 96 % conversion and hence $X_n=25$ is achieved after 18 h (**2a**) and 19 h (**2b**) while the ¹H NMR signals of the monomers have completely disappeared after 40 h (Figure S53, Supporting Information). In view of the exponential increase of X_n in step-growth polymerization,^[10,29,30] confirmed by plotting X_n over the reaction time (see Supporting Information), the degree of polymerization of the soluble digermene polymers **3a,b** must be substantially higher than 25. The inherently large standard deviation close to full conversion (with X_n approaching infinity) is prohibitive regarding an exact value for X_n based on this method.

Despite the high solubility in hydrocarbon and etheric solvents, separation of the polymers **3a,b** from the Tip₂Ge=GeTip₂ by-product is possible by precipitation with acetonitrile from a toluene solution at room temperature (**3a**) and –55 °C (**3b**; for details see Supporting Information). As typical for dissolving polymers,^[31] it takes about a day (depending on the desired concentration) at room temperature to obtain slightly viscous yellow solutions of poly(digermenes) **3a,b** in different solvents. Most of the broad peaks in the solution ¹H NMR spectra (Figure 3) appear at similar shifts as those of the corresponding monomers. Apart from the polymer broadening of the resonances, the main difference between the ¹H NMR spectra of **3a,b** and of the monomers **2a,b** is the significant highfield shift of the resonances of the phenylene linkers by about 1 ppm (**2a**: 8.28, **2b**: 8.36, **3a**: 7.3, **3b**: 7.4 ppm).

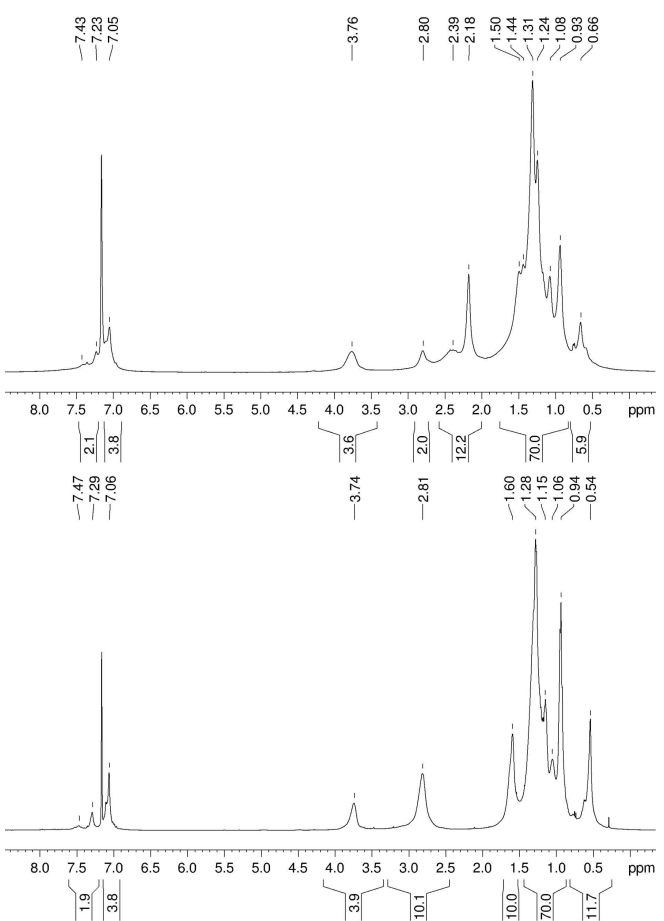


Figure 3. ¹H NMR spectra of 76 g L^{−1} C₆D₆ solutions of poly(digermene)s **3a** (top) and **3b** (bottom), corresponding to repeat unit concentrations of c(**3a**) = 74 and c(**3b**) = 68 mol L^{−1}. Given a detection limit of 50 μM, the absence of Tip₂Ge end group signals suggests minimum degrees of polymerization of 1400.

Considering that the metathetic elimination of the diarylgermylene fragment GeTip₂ and its replacement by the Si-bonded germylene terminus of the polymer chain is separated from the phenylene hydrogen atoms by no less than five bonds, the pronounced shielding is a clear indication of a conjugation effect across the polymer chain, namely σ,π-conjugation involving σ*-orbitals at the silylene linkers. The donation of electron density to the Si centers receives further support from the ²⁹Si NMR resonances of both polymers, which are upfield shifted by 8.0 to 10 ppm compared to the corresponding monomer resonances (**2a**: 7.28, 7.12; **2b**: 7.19; **3a**: –0.91; **3b**: –2.76 ppm).

The NMe₂ and SiMe proton resonances of the Si-octylated derivative **3a** exhibit small shoulders, which are tentatively attributed to the presence of different diastereomers of the polymer owing to the stereogenic centers at the silicon atoms. Integration of all peaks agrees particularly well with the number of protons in the repeat units hence suggesting a remarkably low amount of Tip₂Ge end groups. In fact, assuming a detection limit of 50 μM, the corresponding peaks should be detectable at polymerization degrees smaller than 1400. Their absence is hence consistent with

the formation of near-infinite polymer chains^[32] as suggested by the ¹H NMR spectroscopic monitoring of the conversion (vide supra).

The ¹³C NMR signals of **3a,b** at similar chemical shifts as in the monomers are mostly quite broad with the exception of those assigned to the methyl and methylene groups of the longer alkyl side chains. The latter are remarkably sharp, confirming that they are less prone to the electronic influence of polymer chain. ¹³C and ²⁹Si CP/MAS NMR spectra confirm the structural integrity of the polymers in the solid state (see Supporting Information).

Delocalization along the polymer main chain is further supported by second order perturbation analysis at the BP86/def2-TZVPP level of theory on digermene **4**, serving as model compound for the repeat units of polymers **3a,b**. The optimized geometry of **4** agrees well with the experimental one, exhibiting only minor variations in the bond lengths and angles. The $\pi(\text{Ge}=\text{Ge})$ bond (NBO 96, see Supporting Information Figure S70 for NBO plots) donates into the σ^* -orbitals of the Si–C bonds (NBO 247: 1.51 kcal mol⁻¹; NBO 249: 2.28 kcal mol⁻¹). The phenylene linker (NBO 142) interacts with the σ^* -orbital of the Ge–Si bond (NBO 243: 2.14 kcal mol⁻¹). Additional $\sigma \rightarrow \sigma^*$ conjugation is reflected by stabilization energies of 2.54 kcal mol⁻¹ and 1.92 kcal mol⁻¹, respectively, for the interactions between the Ge–Si and Ge–Ge σ -bonds (NBOs 93 and 95) and the corresponding σ^* -orbitals (NBOs 243 and 245). These conjugative interactions result in relatively low occupancies of the σ - and π -components of the Ge=Ge double bond of 1.92e and 1.85e and the Ge–Si σ -orbital (1.91e).

In line with the yellow color, the UV/Vis longest wavelength absorptions of poly(digermenes) **3a,b** in hexane are observed at $\lambda_{\text{max}} = 423$ nm (**3a**) and 418 nm (**3b**), respectively (Figure 4). These values fall into the typical range of absorptions for $\pi-\pi^*$ transitions of moderately to untwisted acyclic digermenes (411 to 438 nm).^[7c,8–10,11a,d,33,34] TD-DFT calculations on symmetric model digermene **4** at the PBE0/def2-TZVP level of theory confirm the assignment. Compared to model digermene **4** ($\lambda_{\text{max}} = 411$ nm),^[10] they are red-shifted by $\Delta\lambda = 12$ and 7 nm. The onsets of the peaks at 463 nm (**3a**) and 457 nm (**3b**) correspond to HOMO-LUMO gaps of 2.68 and 2.72 eV, respectively, at the lower end of the range of organic π -conjugated materials typically used in OLEDs, OSCs and OFETs (2.64 to 4.01 eV).^[35] Compared to the monomers (both 431 nm) a slight hypsochromic shift is manifest, most likely owing to diminished twisting of the substituents at the Ge=Ge double bond.^[11c,33,36] The weak bands at 334 nm (**3a**) and 338 nm (**3b**) as well as the intense UV bands at ~248 nm and ~295 nm (for both **3a,b**) arise from charge transfer transitions of the Ge=Ge double bond to the linking unit's π -system, according to TD-DFT calculations (see Supporting Information). They are considerably bathochromically shifted compared to the corresponding bands of model digermene **4** (322 nm, 250 nm)^[10] and the σ,π -conjugated monomers (**2a**: 324, 237 nm, **2b**: 322, 237 nm).

As a result of increased stability brought about by σ,π -conjugation, digermene polymers **3a,b** do not react with 1,3-

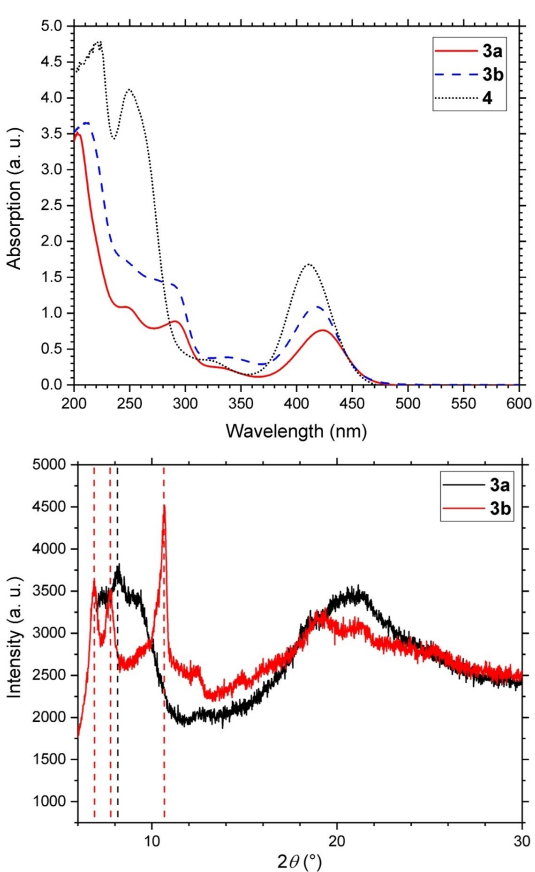


Figure 4. Top: UV/Vis absorption spectra of digermene polymers **3a** (red, solid line; $c = 0.4 \text{ g L}^{-1}$), **3b** (blue, dashed line; $c = 0.9 \text{ g L}^{-1}$) and molecular model **4**^[10] (black; dotted line, $c = 6 \cdot 10^{-4} \text{ M}$). Bottom: Powder X-ray diffractograms of poly(digermene)s **3a,b**.

diisopropylimidazol-4,5-dimethyl-2-ylidene (Me₂IPr) even at 65 °C—unlike monomers **2a,b**. According to heteronuclear NMR spectroscopy, the latter readily react with Me₂IPr at room temperature to form the corresponding bridged bis(germylene)-NHC adducts **5a,b** and Tip₂Ge–NHC, in analogy to the previously reported reaction of Si,Si,N,N-tetramethyl bis(digermene) **2c** to NHC-bis(germylene) **5c** (Scheme 2).^[20] The characteristic ¹³C NMR resonances of the carbenic carbon atoms of **5a,b** are observed between 177.0 and 177.2 ppm as well as particularly broad ¹H NMR signals between 6.3 and 5.2 ppm for the CH backbone of the germylene coordinated carbene. The ²⁹Si NMR signals at -7.16 to -9.94 ppm are characteristically upfield shifted by 14 to 17 ppm compared to preceding bis(digermene)s **2a,b**, similarly to the reported case of **5c** ($\Delta\delta = 15$ –16 ppm).^[20] For the Si-octylated derivative **5a**, the presence of several diastereomers in the mixture is expected due to four stereogenic centers, in line with broad multiplets in the corresponding heteronuclear NMR spectra.

Conjugated polymers find applications as semiconducting thin film materials in electronic devices. For efficient charge transport, ordered structures are required.^[2,37] We therefore investigated the deposition behavior of polymers **3a,b** and the morphology of resulting thin films. Noticeably,

powder X-ray diffraction of the bulk samples of polymers **3a,b** (Figure 4) revealed partial crystallinity, demonstrating a relatively high level of order. Particularly in the case of the *N*-hexyl derivative **3b**, several distinct reflections of significant intensity are observed at $2\theta=6.9^\circ$ (1.28 nm), 7.7° (1.15 nm) and 10.7° (0.83 nm). The *Si*-octyl substituted poly(digermene) **3a** appears to show a lower degree of crystallinity as suggested by only one distinct peak protruding at 8.2° (1.08 nm) from the otherwise very broad reflections in smaller 2θ values.

The amorphous contributions to both diffractograms resemble those of ladder structures of amorphous polysilsesquioxanes exhibiting characteristic broad reflections at $2\theta \sim 20^\circ$ ($d=0.34$ to 0.53 nm) in addition to those at smaller 2θ angles.^[38] The short distance of 0.83 nm is assigned to intramolecular distances between the Ge=Ge units, which is slightly smaller than the value estimated from the single crystal structure of monomer **2b** (1.00 nm). The larger values are assigned to interstrand Ge–Ge distances, fitting the lower end of the corresponding values derived from the molecular solid-state structures (**2a**: 1.15–1.66 nm, **2b**: 1.05–1.69 nm). In line with this, the monomers show relatively short distances between adjacent molecules, in particular between the alkyl chains with H–H distances as short as 2.7651(2) Å (**2a**) and 3.2687(2) Å (**2b**) and the isopropyl groups of the Tip substituents with H–H distances of 1.9347(1) Å (**2a**) and 2.1659(1) Å (**2b**). We assume that the resulting mutual penetration of two molecules via London dispersion interactions between the alkyl branches (Figure 1b) is retained in the polymeric structures **3a,b** along individual strands. The resulting ladder structures could account for the larger 2θ values ($d=0.34$ to 0.53 nm) exhibited in the powder XRD patterns.

The presence of interchain interactions is evident in the formation of highly viscous gels when the polymerization is performed at higher monomer concentrations or upon slow evaporation of the solvent of polymer solutions. In addition to a high degree of polymerization, this is expected to result in an increase of the general stiffness of the compounds and hence in higher glass transition temperatures.^[39,40] Indeed, in contrast to the *Si,Si,N,N*-tetramethyl substituted digermene polymer **IV**, which exhibits a T_g of 72°C,^[10] no glass transitions are obtained for **3a,b** in the temperature range between –40°C and 160°C. The constitutional integrity of the polymers after heating to 160°C in the solid state was confirmed by ¹H NMR spectroscopy of dissolved samples with no discernible changes compared to pristine samples. At higher temperatures, degradation of **3a,b** is observed: heating solid samples of **3a,b** to 200°C for 1.5 h results in the appearance of additional sharp ¹H NMR signals in solution spectra (**3b**) or the formation of an insoluble solid (**3a**). This is in line with additional exothermic DSC events at onset temperatures of 167°C (**3a**) and 168°C (**3b**), respectively (Figure 5).

At room temperature and in the absence of air and moisture, the polymers are stable for at least two years in the solid state and in solution, according to ¹H NMR spectroscopy. When exposed to air, rapid degradation of **3a** and **3b** to unknown molecular fragments is observed.

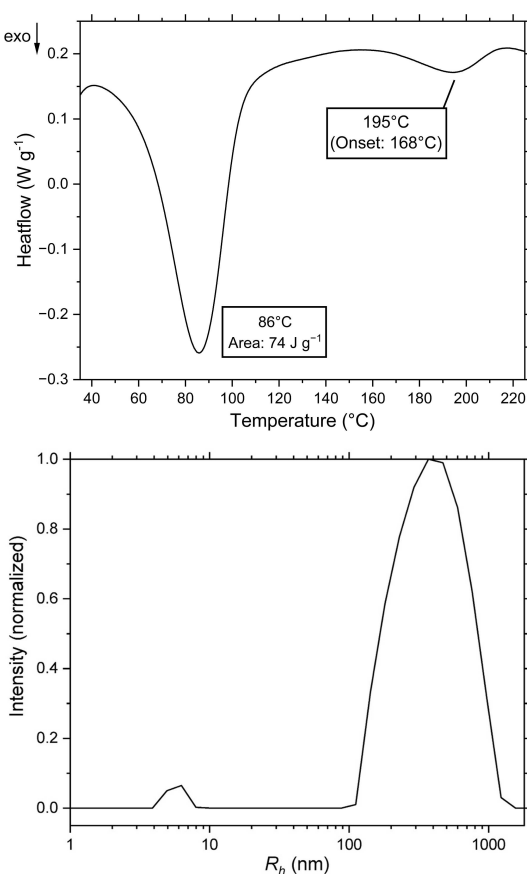


Figure 5. Top: DSC curve of digermene polymer **3b** recorded at 10 K min⁻¹. Bottom: Size distribution profile obtained from DLS measurement of **3a** in benzene at a scattering angle of 25°.

Melting of the samples in NMR tubes was only observed well above the degradation temperatures at 242°C (**3a**) and 250°C (**3b**). The melting temperatures exceed by far those of the monomers (**2b**: 160°C; **2c**: 180°C), in line with the increased stiffness. According to thermal gravimetric analyses (TGA), the melting processes are accompanied by mass loss. The corresponding onset temperatures (**3a**: 243°C, **3b**: 249°C) are substantially higher than for the *Si,Si,N,N*-tetramethyl derivative **IV** (122°C),^[10] confirming the considerable stabilization brought about by the intermolecular dispersive interactions of the alkyl chains and the vastly higher degrees of polymerization in polymers **3a,b**. Furthermore, the first cycles of the DSC measurements (Figure 5 and Supporting Information) reveal remarkably intense irreversible exothermal events at 81–82°C (**3a**) and 86–96°C (**3b**), tentatively attributed to the increased order by the establishment of additional interchain interactions and hence supramolecular structures. The heat release corresponding to energies of 37–48 J g⁻¹ (**3a**) and 74–75 J g⁻¹ (**3b**) is in line with heat-induced crystallization processes.^[41]

The formation of aggregates of sizes of at least 150 nm is confirmed by small angle X-ray scattering (SAXS) experiments on concentrated (30 to 45 g L⁻¹) solutions of **3a,b** in toluene (Figure S86, Supporting Information), showing strong forward scattering. Furthermore, the forward scatter-

ing in the case of *Si*-octylated poly(digermene) **3a** follows a slope close to q^{-1} at intermediate scattering vector values ($q=0.02\text{--}0.1 \text{\AA}^{-1}$) and for **3b** a trend towards q^{-1} is found. The corresponding mass-fractal dimension of $D_m=1$, indicative of elongated structures,^[42] is consistent with the presence of cylindrical particles.

Hydrodynamic radii obtained with dynamic light scattering (DLS) experiments (Figure 5 and Supporting Information) on 5 g L⁻¹ benzene solutions of the polymers show a strong scattering angle dependency, characteristic for large or anisotropically shaped particles above the Rayleigh limit.^[43a,e,44] The hydrodynamic radii at $R_h=5.3 \text{ nm}$ (**3a**) and 4.8 nm (**3b**) correspond to diffusion coefficients (**3a**: $D=6.8\cdot10^{-11}$, **3b**: $D=7.6\cdot10^{-11} \text{ m}^2\text{s}^{-1}$) in the range of translational diffusion of high-molecular-weight polymer chains (polystyrenes with $M_w=30000$ to 200000 g mol⁻¹ exhibit values of $D=8$ to $3\cdot10^{-11} \text{ m}^2\text{s}^{-1}$)^[45] and expectedly about one order of magnitude smaller compared to rod-like polymers with correspondingly larger volumes such as cellulose or the tobacco mosaic virus ($D=1.5\cdot10^{-12}$ to $6.0\cdot10^{-12} \text{ m}^2\text{s}^{-1}$).^[44b,46] The peaks at higher radii (**3a**: 389 nm, **3b**: 168 nm) are in line with the presence of supramolecular structures with approximately $10^7\text{--}10^8$ repeat units per agglomerate (for details see Supporting Information).

Diffusion ordered NMR spectroscopy (DOSY) on 10 g L⁻¹ solutions in THF-*d*₈ provided two different diffusion coefficients for each derivative (for details see Supporting Information). The smaller diffusion coefficients of $D=4.4\cdot10^{-11}$ (**3a**) and $5.2\cdot10^{-11} \text{ m}^2\text{s}^{-1}$ (**3b**) are one order of magnitude smaller than the values obtained for the monomers (**2a**: $D=5.4\cdot10^{-10} \text{ m}^2\text{s}^{-1}$, $R_h=0.84 \text{ nm}$; **2b**: $D=5.0\cdot10^{-10} \text{ m}^2\text{s}^{-1}$, $R_h=0.91 \text{ nm}$), accounting for considerably larger volumes, in the same order of magnitude as single polymer strand translational diffusion observed in the DLS experiments (**3a**: $D=6.8\cdot10^{-11}$, **3b**: $D=7.6\cdot10^{-11} \text{ m}^2\text{s}^{-1}$). The larger diffusion coefficients (**3a**: $D=1.3\cdot10^{-10} \text{ m}^2\text{s}^{-1}$; **3b**: $D=1.4\cdot10^{-10} \text{ m}^2\text{s}^{-1}$) are tentatively assigned to slow rotational diffusion processes about rotational axes perpendicular to the main axis of the approximately cylindrically shaped polymer strands. Similar conclusions have been drawn for rod-like particles typically formed by *para*-phenylene-containing repeat units.^[43,47] Using a modified version of the Stokes-Einstein equation for cylindrical structures with widths corresponding to the monomers' diameters (see Supporting Information for details), the translational diffusion coefficients allow for a tentative rod length estimation of 2100 nm (**3a**) and 1100 nm (**3b**), respectively. Assuming the rods to consist of unentangled polymer chains with strict linear conformation and a repeat unit length of 1 nm (estimated from the distances between two Ge=Ge moieties in the molecular structures of **2a,b**), these lengths suggest degrees of polymerization X_n of similar absolute values. The corresponding molecular weights amount to 2200 and 1400 kg mol⁻¹.

The presence of large cylindrical superstructures of **3a,b** in solution and in the solid state due to the attractive dispersion forces between the alkyl side-chains of different polymer strands prompted us to investigate the deposition of highly ordered thin films. A concentrated hexane solution

of the *N*-hexylated derivative **3b** (1 g L⁻¹) was spin-coated onto a mica substrate and the surface was scanned using atomic force microscopy (AFM). The resulting image shows the substrate covered by a layer (thickness 12 to 18 nm) of the polymer and randomly distributed crystalline peaks protruding about 14 to 29 nm from the relatively soft amorphous background (Figure 6a). Thinner films with more clearly defined nanostructures, are obtained from less concentrated solutions (0.4 g L⁻¹) by dip-coating and subsequent washing with hexane. A mica substrate coated with *Si*-octylated polymer **3a** (Figure 6b) exhibits a pattern of approximately parallel long strands, confirming the formation of cylindrical superstructures as presumed on the basis of the solution and solid state analytical data.

Close-ups at higher resolution reveal the strands to be about 500 nm in breadth (Figure 6c and Supporting Infor-

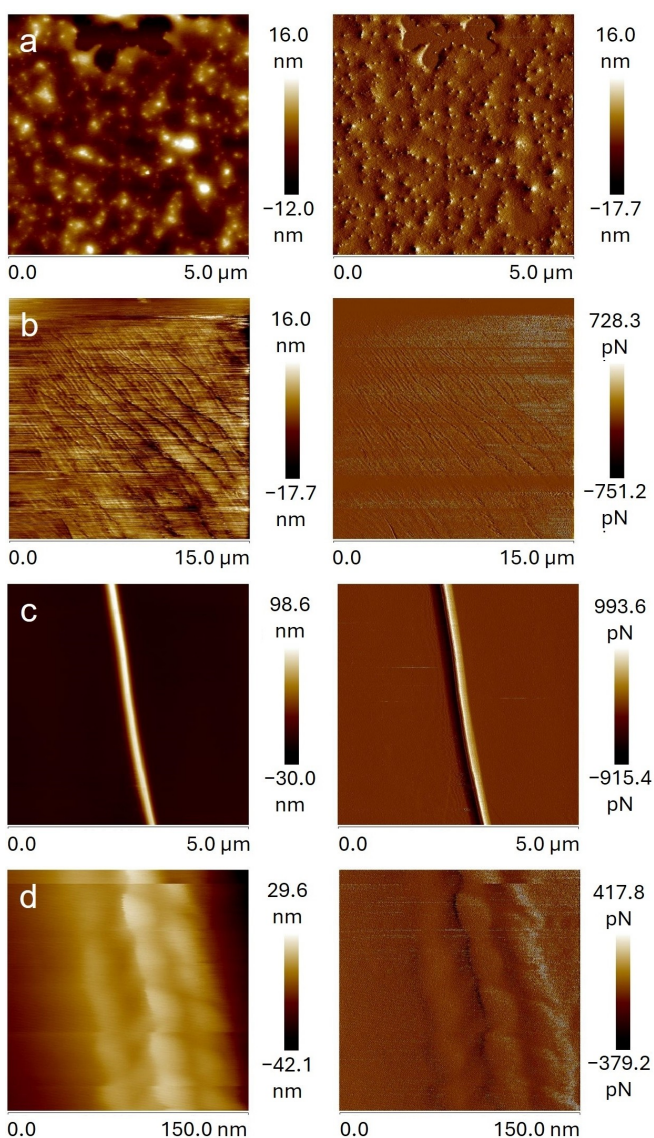


Figure 6. AFM images of a) **3b** spin-coated with a 1 g L⁻¹ hexane solution and b-d) **3a** dip-coated with a 0.4 g L⁻¹ hexane solution on mica substrates (left: height sensor, right: peak force error).

mation Figure S96). Similar rods formed by the *N*-hexylated derivative on a highly ordered pyrolytic graphite (HOPG) surface are thinner with a width of about 64 nm (Figures S95, S96, Supporting Information). The orientation of these rods in the thin films implies an ordering along the conjugation path parallel to the surface. Notably, the rods are between five and ten times flatter than wide with heights of 97 nm (**3a**) and 6.4 nm (**3b**) (Figure S96, Supporting Information). The agglomerates hence exhibit an almost sheet-like shape consisting of several parallel adjacent fibrils.

At closer view, a plait-like structure of the strands becomes apparent in the case of the *Si*-octylated derivative **3a** (Figure 6d). This repetitive pattern suggests an ordered arrangement of the cylindrical agglomerates and consequently of the underlying polymer chains, in line with regular attractive interactions between the single chains and even between adjacent fibrils as known for instance from polyacrylonitrile fibers.^[48]

Transmission electron microscopy (TEM) of both derivatives was performed on samples on holey carbon-coated copper TEM grids, prepared by drop-coating hexane or toluene solutions. In line with the AFM findings, the resulting images (Figure 7a and Supporting Information) show broad bundles of polymers in the case of concentrated solutions (1 g L^{-1}) with an approximate width of 50 nm. More dilute poly(digermene) solutions result in numerous parallel fibrils each of a width of about 3 nm (Figure 7b–d and Supporting Information). The width of individual polymer chains of **3a,b** is estimated to about 1.6–1.8 nm on the basis of the DOSY data and the crystal structures of

monomers **2a,b** (see also Supporting Information). Hence, the observed fibrils most probably show ladder structures consisting of two interlocked polymer strands resulting in a theoretical width $< 3.6 \text{ nm}$.

Their linear parallel alignment corroborates the assumed self-assembly due to distinct interchain interactions and a general rigidity of the linear chains. Cross-linked cylindrical micelles of poly(ferrocenylsilane) block copolymers, for instance, assemble in a parallel manner resulting in supramolecular fibers.^[49] Notably, the lamellar substructures in the poly(digermene) films resemble the well-ordered structures of regioregular poly(thiophene)s used in organic solar cells and field effect transistors.^[50] The images in Figures 7b,c additionally show regions with mesh-like structures (see also Figure S97, Supporting Information), suggesting an overlay of several crossing fibers. Such patterns may result from a different morphology, e.g. as in fringed micelles where the ends of parallel polymer strands form knots.^[48,51,52]

Conclusions

In conclusion, polymers with Ge=Ge double bonds in the conjugation path and extremely high degrees of polymerization have been synthesized and characterized in solution, as bulk solids and in thin films. By equipping the silylene-phenylene bridge between the Ge=Ge moieties with long alkyl chains either at the silyl group or the amino functionality, considerable solubility in different organic solvents is conferred. This allows for essentially unlimited chain growth in the polymerization process following our recently reported HADMET protocol for the metathesis of bis(digermene)s. Substantial intermolecular dispersion interactions between the alkyl groups of adjacent polymer chains lead to the formation of ladder-like cylindrical assemblies in solution and in thin films as apparent from AFM and TEM images and corroborated by diffusion experiments and powder XRD. The thin films exhibit ordered structures of parallel aligned fibrils, consistent with the partial crystallinity of the bulk polymer, which ultimately results in a reasonable thermal stability of the Ge=Ge-containing polymers up to $> 160^\circ\text{C}$. Characterization of the bis(digermene) monomers supported by DFT calculations confirms substantial σ,π -conjugation across the silylene-phenylene linker and the Ge=Ge units. This is further corroborated by the NMR and UV/Vis data of the yellow polymer solutions. In combination with the absorption in the visible range, due to a small HOMO–LUMO gap, this new class of materials offers interesting perspectives for the application in polymer electronics.

Supporting Information

The authors have cited additional references within the Supporting Information (Ref. [54–77]).

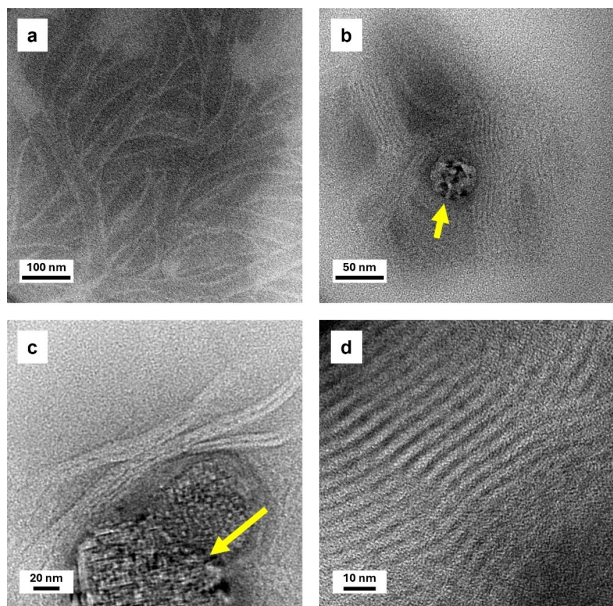


Figure 7. TEM images showing the morphologies of supramolecular structures formed by poly(digermene)s on holey carbon-coated copper grids prepared by drop-coating of polymer solutions of different concentrations: a) **3b** ($c = 1 \text{ g L}^{-1}$), b) **3a** (0.1 g L^{-1}), c) **3b** (0.4 g L^{-1}), d) **3a** (0.1 g L^{-1}). Yellow arrows mark areas where mesh-like structures are exhibited.

Acknowledgements

We thank the Fonds der Chemischen Industrie for a Kekulé fellowship for A.-L.T. and the German Research Foundation for funding (DFG SCHE 906/9-1). We acknowledge the instrumentation facilities provided by the service center for X-ray analysis established with the financial support from Saarland University and German Research Foundation (INST 256/506-1). We thank Diego M. Andrada for access to his computational cluster. We are grateful for measurements by Michael Zimmer, Elias Gießelmann (Solid State CP/MAS NMR), Josef Zapp (DOSY NMR), Lucas Niedner (DLS), Jörg Schmauch (TEM), Bastian Oberhausen and Jan-Falk Kannengießer (DSC), Mana Mohamed (TGA) and for preliminary experiments by Lukas Klemmer. Open Access funding enabled and organized by Projekt DEAL.

Conflict of Interest

The authors declare no conflict of interest.

Data Availability Statement

The data that support the findings of this study are available in the supplementary material of this article.

Keywords: conjugated polymers · thin films · σ,π -conjugation · self-assembly · dispersion interactions

- [1] a) H. F. Brinson, L. C. Brinson, in *Polymer Engineering Science and Viscoelasticity*, Springer, New York **2015**; b) T. D. Clemens, S. I. Stupp, *Prog. Polym. Sci.* **2020**, *111*, 101310; c) M. Zakaria, M. A. R. Bhuiyan, M. S. Hossain, N. M.-M. U. Khan, M. A. Salam, K. Nakane, *Discover Nano* **2024**, *19*, 24; d) Y. Wang, H. Li, A. Rasool, H. Wang, R. Manzoor, G. Zhang, *J. Nanobiotechnol.* **2022**, *24*, 1; e) L. Guo, Y. Wang, M. Steinhart, *Chem. Soc. Rev.* **2021**, *50*, 6333; f) W. Hou, Y. Xiao, G. Han, J.-Y. Lin, *Polymers* **2019**, *11*, 143; g) F. R. R. Teles, L. P. Fonseca, *Mater. Sci. Eng. C* **2008**, *28*, 1530; h) P. Das, P. K. Marvi, S. Ganguly, X. S. Tang, B. Wang, S. Srinivasan, A. R. Rajabzadeh, A. Rosenkranz, *Nano-Micro Lett.* **2024**, *16*, 135; i) E. Tamjid, P. Najafi, M. A. Khalili, N. Shokouhnejad, M. Karimi, N. Sepahdoost, *Discover Nano* **2024**, *19*, 29.
- [2] Reviews: a) K. Müllen, U. Scherf, *Macromol. Chem. Phys.* **2023**, *224*, 2200337; b) M. C. Scharber, N. S. Sariciftci, *Adv. Mater. Technol.* **2021**, *6*, 2000857; c) G. Hong, X. Gan, C. Leonhardt, Z. Zhang, J. Seibert, J. M. Busch, S. A. Bräse, *Adv. Mater.* **2021**, *33*, 2005630; d) R. H. Friend, R. W. Gymer, A. B. Holmes, J. H. Burroughes, R. N. Marks, C. Taliani, D. D. Bradley, D. A. Dos Santos, J. L. Brédas, M. Lögdlund, W. R. Salaneck, *Nature* **1999**, *397*, 121.
- [3] S. Fratini, M. Nikolka, A. Salleo, G. Schweicher, H. Sirringhaus, *Nat. Mater.* **2020**, *19*, 491.
- [4] a) R. R. Moskalyk, *Miner. Eng.* **2004**, *17*, 393; b) E. Rosenberg, *Rev. Environ. Sci. Bio/Technol.* **2009**, *8*, 29; c) M. Patel, A. K. Karamalidis, *Sep. Purif. Technol.* **2021**, *275*, 118981.
- [5] a) B. L. Lucht, M. A. Buretea, T. Don, *Organometallics* **2000**, *19*, 3469; b) N. Allard, R. B. Aich, D. Gendron, P.-L. T. Boudreault, C. Tessier, S. Alem, S.-C. Tse, Y. Tao, M. Leclerc,
- [6] Reviews: a) P. P. Power, *J. Chem. Soc. Dalton Trans.* **1998**, 2939; b) P. P. Power, *Chem. Rev.* **1999**, *99*, 3463; c) R. C. Fischer, P. P. Power, *Chem. Rev.* **2010**, *110*, 3877; d) R. C. Fischer, in *Comprehensive Inorganic Chemistry II*, Vol. 2 (Eds.: J. Reedijk, K. Poeppelmeier), Elsevier, Waltham, MA, USA **2013**, pp. 269; e) V. Nesterov, N. C. Breit, S. Inoue, *Chem. Eur. J.* **2017**, *23*, 12014; f) C. Weetman, *Chem. Eur. J.* **2021**, *27*, 1941; g) F. Dankert, C. Hering-Junghans, *Chem. Commun.* **2022**, *58*, 1242; h) S. Fujimori, Y. Mizuhata, N. Tokitoh, *Proc. Jpn. Acad. Ser. B* **2023**, *99*, 480; i) V. Y. Lee, *Molecules* **2023**, *28*, 1558; j) C. Duan, C. Cui, *Chem. Soc. Rev.* **2024**, *53*, 361.
- [7] a) S. Masamune, Y. Hanzawa, D. J. Williams, *J. Am. Chem. Soc.* **1982**, *104*, 6136; b) P. B. Hitchcock, M. F. Lappert, S. J. Miles, A. J. Thorne, *J. Chem. Soc. Chem. Commun.* **1984**, 480; c) J. Park, S. A. Batcheller, S. Masamune, *J. Organomet. Chem.* **1989**, *367*, 39; d) H. Schäfer, W. Saak, M. Weidenbruch, *Organometallics* **1999**, *18*, 3159; e) M. Stender, L. Pu, P. P. Power, *Organometallics* **2001**, *20*, 1820; f) K. L. Hurni, P. A. Rupar, N. C. Payne, K. M. Baines, *Organometallics* **2007**, *26*, 5569; g) T. J. Hadlington, M. Hermann, J. Li, G. Frenking, C. Jones, *Angew. Chem. Int. Ed.* **2013**, *52*, 10199; h) N. Hayakawa, T. Sugahara, Y. Numata, H. Kawai, K. Yamatani, S. Nishimura, S. Goda, Y. Suzuki, T. Tanikawa, H. Nakai, D. Hashizume, T. Sasamori, N. Tokitoh, T. Matsuo, *Dalton Trans.* **2018**, *47*, 814; i) K. Suzuki, Y. Numata, N. Fujita, N. Hayakawa, T. Tanikawa, D. Hashizume, K. Tamao, H. Fueno, K. Tanakade, T. Matsuo, *Chem. Commun.* **2018**, *54*, 2200.
- [8] D. Nieder, L. Klemmer, Y. Kaiser, V. Huch, D. Scheschkeiwitz, *Organometallics* **2018**, *37*, 632.
- [9] X. Zheng, A. E. Crumpton, M. A. Ellwanger, S. Aldridge, *Dalton Trans.* **2023**, *52*, 16591.
- [10] L. Klemmer, A.-L. Thömmes, M. Zimmer, V. Huch, B. Morgenstern, D. Scheschkeiwitz, *Nat. Chem.* **2020**, *13*, 373.
- [11] a) M. Kira, T. Iwamoto, T. Maruyama, C. Kabuto, H. Sakurai, *Organometallics* **1996**, *15*, 3767; b) A. Schäfer, W. Saak, M. Weidenbruch, *Z. Anorg. Allg. Chem.* **1998**, *624*, 1405; c) V. Y. Lee, K. McNeice, Y. Ito, A. Sekiguchi, *Chem. Commun.* **2011**, *47*, 3272; d) L. Klemmer, Y. Kaiser, V. Huch, M. Zimmer, D. Scheschkeiwitz, *Chem. Eur. J.* **2019**, *25*, 12187; e) K. Izod, M. Liu, P. Evans, C. Wills, C. M. Dixon, P. G. Waddell, M. R. Probert, *Angew. Chem. Int. Ed.* **2022**, *61*, e202208851; f) A. Caise, L. P. Griffin, A. Heilmann, C. McManus, J. Campos, S. Aldridge, *Angew. Chem. Int. Ed.* **2021**, *60*, 15606.
- [12] a) C. Cui, M. M. Olmstead, P. P. Power, *J. Am. Chem. Soc.* **2004**, *126*, 5062; b) T. Sasamori, T. Sugahara, T. Agou, J.-D. Guo, S. Nagase, R. Streubel, N. Tokitoh, *Organometallics* **2015**, *34*, 2106; c) T. Sugahara, J.-D. Guo, T. Sasamori, Y. Karatsu, Y. Furukawa, A. E. Ferao, S. Nagase, N. Tokitoh, *Bull. Chem. Soc. Jpn.* **2016**, *89*, 1375.
- [13] a) C. Prässang, D. Scheschkeiwitz, *Chem. Soc. Rev.* **2016**, *45*, 900; b) A. Rammo, D. Scheschkeiwitz, *Chem. Eur. J.* **2018**, *24*, 6866.
- [14] a) D. Scheschkeiwitz, *Chem. Lett.* **2011**, *40*, 2; b) T. Matsuo, N. Hayakawa, *Sci. Technol. Adv. Mater.* **2018**, *19*, 108.
- [15] a) D. Scheschkeiwitz, *Angew. Chem. Int. Ed.* **2004**, *43*, 2965; b) M. Ichinohe, K. Sanuki, S. Inoue, A. Sekiguchi, *Organometallics* **2004**, *23*, 3088; c) M. Ichinohe, K. Sanuki, S. Inoue, A. Sekiguchi, *Silicon Chem.* **2005**, *3*, 111; d) S. Inoue, M. Ichinohe, A. Sekiguchi, *Chem. Lett.* **2005**, *34*, 1564; e) T. Iwamoto, M. Kobayashi, K. Uchiyama, S. Sasaki, S. Nagendran, S. Isobe, M. Kira, *J. Am. Chem. Soc.* **2009**, *131*, 3156; f) L. Zborovsky, R.

- Dobrovetsky, M. Botoshansky, D. Bravo-Zhivotovskii, Y. Apeloig, *J. Am. Chem. Soc.* **2012**, *134*, 18229; g) D. Pinchuk, J. Mathew, A. Kaushansky, D. Bravo-Zhivotovskii, Y. Apeloig, *Angew. Chem. Int. Ed.* **2016**, *55*, 10258; h) A. Rit, J. Campos, H. Niu, S. Aldridge, *Nat. Chem.* **2016**, *8*, 1022; i) M. Tian, J. Zhang, H. Yang, C. Cui, *J. Am. Chem. Soc.* **2020**, *142*, 4131; j) P. K. Majhi, V. Huch, D. Scheschkewitz, *Angew. Chem. Int. Ed.* **2021**, *60*, 242.
- [16] I. Bejan, D. Scheschkewitz, *Angew. Chem. Int. Ed.* **2007**, *46*, 5783.
- [17] a) A. Fukazawa, Y. Li, S. Yamaguchi, H. Tsuji, K. Tamao, *J. Am. Chem. Soc.* **2007**, *129*, 14164; b) L. Li, T. Matsuo, D. Hashizume, H. Fueno, K. Tanaka, K. Tamao, *J. Am. Chem. Soc.* **2015**, *137*, 15026.
- [18] N. M. Obeid, L. Klemmer, D. Maus, M. Zimmer, J. Jeck, I. Bejan, A. J. P. White, V. Huch, G. Jung, D. Scheschkewitz, *Dalton Trans.* **2017**, *46*, 8839.
- [19] T. Kosai, S. Ishida, T. Iwamoto, *Dalton Trans.* **2017**, *46*, 11271.
- [20] A.-L. Thömmes, B. Morgenstern, M. Zimmer, D. M. Andrade, D. Scheschkewitz, *Chem. Eur. J.* **2023**, *29*, e202301273.
- [21] A. M. Priegert, B. W. Rawe, S. C. Serin, D. P. Gates, *Chem. Soc. Rev.* **2016**, *45*, 922.
- [22] a) V. A. Wright, D. P. Gates, *Angew. Chem. Int. Ed.* **2002**, *41*, 2389; b) R. C. Smith, X. Chen, J. D. Protasiewicz, *Inorg. Chem.* **2003**, *42*, 5468.
- [23] R. C. Smith, J. D. Protasiewicz, *J. Am. Chem. Soc.* **2004**, *126*, 2268.
- [24] J.-P. Malrieu, G. Trinquier, *J. Am. Chem. Soc.* **1989**, *111*, 5916.
- [25] W. Ando, H. Ito, T. Tsumuraya, H. Yoshida, *Organometallics* **1988**, *7*, 1880.
- [26] H. Maeda, T. Suzuki, M. Segi, *Photochem. Photobiol. Sci.* **2018**, *17*, 781.
- [27] a) M.-C. Fang, A. Watanabe, M. Matsuda, *Jpn. J. Appl. Phys.* **1995**, *34*, 98; b) S. Kyushin, M. Ikarugi, M. Goto, H. Hiratsuka, H. Matsumoto, *Organometallics* **1996**, *15*, 1067; c) S. Kyushin, T. Kitahara, H. Matsumoto, *Chem. Lett.* **1998**, *27*, 471; d) S. Kyushin, T. Matsuura, H. Matsumoto, *Organometallics* **2006**, *25*, 2761; e) S. Kyushin, Y. Suzuki, *Molecules* **2022**, *27*, 2241.
- [28] J. P. Wagner, P. R. Schreiner, *Angew. Chem. Int. Ed.* **2015**, *54*, 12274.
- [29] W. H. Carother, *Trans. Faraday Soc.* **1936**, *32*, 39.
- [30] H. G. Elias, *Makromolecules*, Vol. 2, Wiley-VCH GmbH Verlag, Weinheim, Germany **2006**.
- [31] B. A. Miller-Chou, J. L. Koenig, *Prog. Polym. Sci.* **2003**, *28*, 1223.
- [32] The model of infinite chains is widely used for the theoretical description of polymers with considerable degrees of polymerisation (see for instance: a) B. Champagne, J.-M. André, *Int. J. Quantum Chem.* **1990**, *38*, 859; b) D. S. Galvão, M. J. Caldas, *J. Chem. Phys.* **1990**, *92*, 2630; c) J. Kürti, H. Kuzmany, *Phys. Rev. B* **1991**, *44*, 597; d) R. Wang, Z.-G. Wang, *Macromolecules* **2014**, *47*, 4094). Polyiodine chains in an experimentally obtained pyrroloperylene-iodine complex have also been referred to as infinite (see e) S. Madhu, H. A. Evans, V. V. T. Doan-Nguyen, J. G. Labram, G. Wu, M. L. Chabinyc, R. Seshadri, F. Wudl, *Angew. Chem. Int. Ed.* **2016**, *55*, 8032). In view of the essentially unlimited chain growth during polymerization, supported by the discussed NMR spectroscopic data, we refer to the poly(digermene) chains herein as *near-infinite*.
- [33] M. Kira, *Proc. Jpn. Acad. Ser. B* **2012**, *88*, 167.
- [34] T. Iwamoto, J. Okita, N. Yoshida, M. Kira, *Silicon* **2010**, *2*, 209.
- [35] J. C. S. Costa, R. J. S. Taveira, C. F. R. A. C. Lima, A. Mendes, L. M. N. B. F. Santos, *Opt. Mater.* **2016**, *58*, 51.
- [36] V. Y. Lee, K. McNiece, Y. Ito, A. Sekiguchi, N. Geinik, J. Y. Becker, *Heteroat. Chem.* **2014**, *25*, 313.
- [37] a) Y. Lei, P. Deng, M. Lin, X. Zheng, F. Zhu, B. S. Ong, *Adv. Mater.* **2016**, *28*, 6687; b) M. Li, D. K. Mangalore, J. Zhao, J. H. Carpenter, H. Yan, H. Ade, H. Yan, K. Müllen, P. W. M. Blom, W. Pisula, D. M. de Leeuw, K. Asadi, *Nat. Commun.* **2018**, *9*, 451; c) M. Gao, W. Wang, J. Hou, Y. L. Long, *Aggregate* **2021**, *2*, e46.
- [38] a) K. A. Andrianov, S. V. Bushin, M. G. Vitovskaya, V. N. Yemel'yanov, P. N. Lavrenko, N. N. Makarova, A. M. Muzafov, V. Y. Nikolayev, G. F. Kolbina, I. N. Shtennikova, V. N. Tsvetkov, *Polym. Sci. U. S. S. R.* **1977**, *19*, 536; b) C. Liu, Y. Liu, Z. Shen, P. Xie, R. Zhang, J. Yang, F. Bai, *Macromol. Chem. Phys.* **2001**, *202*, 1581; c) K. Deng, T. Zhang, X. Zhang, A. Zhang, P. Xie, R. Zhang, *Macromol. Chem. Phys.* **2006**, *204*, 404; d) X. Zhang, P. Xie, Z. Shen, J. Jiang, C. Zhu, H. Li, T. Zhang, C. C. Han, L. Wan, S. Yan, R. Zhang, *Angew. Chem. Int. Ed.* **2006**, *45*, 3112; e) Z.-X. Zhang, J. Hao, P. Xie, X. Zhang, C. C. Han, R. Zhang, *Chem. Mater.* **2008**, *20*, 1322; f) M. Handke, B. Handke, A. Kowalewska, W. Jastrzebski, *J. Mol. Struct.* **2009**, *254*, 924; g) M. Handke, M. Sitarz, E. Dlugon, *J. Mol. Struct.* **2011**, *993*, 193; h) Z. Chena, Z. Renb, J. Zhang, W. Fua, Z. Lia, R. Zhang, *React. Funct. Polym.* **2012**, *72*, 503; i) S.-S. Choi, A. S. Lee, S. S. Hwang, K.-Y. Baek, *Macromolecules* **2015**, *48*, 6063; j) W. R. Kang, A. S. Lee, S. Park, S.-H. Park, K.-Y. Baek, K. B. Lee, S.-H. Lee, J.-H. Lee, S. S. Hwang, J. S. Lee, *J. Membr. Sci.* **2015**, *475*, 384; k) M. Pei, A. S. Lee, S. S. Hwang, H. Yang, *J. Mater. Chem. C* **2017**, *5*, 10955; l) S. O. Hwanga, A. S. Leeb, J. Y. Leea, S.-H. Parka, K. I. Junga, H. W. Junga, J.-H. Lee, *Prog. Org. Coat.* **2018**, *121*, 105; m) W. Zhang, X. Wang, Y. Wu, Z. Qi, R. Yang, *Inorg. Chem.* **2018**, *57*, 3883; n) S. Pohl, O. Janka, E. Füglein, G. Kickelbick, *Macromolecules* **2021**, *54*, 3873; o) J. Marchewka, P. Jelen, I. Rutkowska, P. Bezko, M. Sitarz, *Materials* **2021**, *14*, 1340.
- [39] a) J. H. Gibbs, E. A. DiMarzio, *J. Chem. Phys.* **1958**, *28*, 373; b) M. C. Shen, A. Eisenberg, *Prog. Solid State Chem.* **1967**, *3*, 407; c) V. P. Privalko, Y. S. Lipatov, *J. Macromol. Sci. Phys.* **1974**, *9*, 551; d) C. Müller, *Chem. Mater.* **2015**, *27*, 2740; e) R. Xie, A. R. Weisen, Y. Lee, M. A. Aplan, A. M. Fenton, A. E. Masucci, F. Kempe, M. Sommer, C. W. Pester, R. H. Colby, E. D. Gomez, *Nat. Commun.* **2020**, *11*, 893.
- [40] H. Domininghaus, P. Elsner, P. Eyerer, T. Hirth, *Kunststoffe – Eigenschaften und Anwendungen*, Springer-Verlag Berlin Heidelberg, Germany **2008**.
- [41] C. Schick, *Anal. Bioanal. Chem.* **2009**, *395*, 1589.
- [42] G. Beaucage, *J. Appl. Crystallogr.* **1996**, *29*, 134.
- [43] a) S. R. Aragón, R. Pecora, *J. Chem. Phys.* **1977**, *66*, 2506; b) S. Fujime, K. Kubota, *Biophys. Chem.* **1985**, *23*, 1; c) R. Piazza, V. Degiorgio, *J. Phys. Condens. Matter* **1993**, *5*, B173; d) D. Lehner, H. Lindner, O. Glatter, *Langmuir* **2000**, *16*, 1689; e) F. Babick, in *Micro and Nano Technologies. Characterization of Nanoparticles* (Eds.: V.-D. Hodoroaba, W. E. S. Unger, A. G. Shard), Elsevier **2020**, pp. 137.
- [44] a) R. Pecora, *J. Chem. Phys.* **1968**, *48*, 4126; b) E. Loh, E. Ralston, V. N. Schumaker, *Biopolymers* **1979**, *18*, 2549; c) H. Kato, A. Nakamura, S. Kinugasa, *Nanomaterials* **2018**, *8*, 708; d) L. Jin, C. W. Jarand, M. L. Brader, W. F. Reed, *Meas. Sci. Technol.* **2022**, *33*, 045202.
- [45] W. Li, H. Chung, C. Daeffler, J. A. Johnson, R. H. Grubbs, *Macromolecules* **2012**, *45*, 9595.
- [46] Y. Boluk, C. Danumah, *J. Nanopart. Res.* **2014**, *16*, 2174.
- [47] H. G. Elias, *Makromolecules*, Vol. 3, Wiley-VCH GmbH Verlag, Weinheim, Germany **2008**.
- [48] C. Kunzmann, G. Schmidt-Bilkenroth, J. Moosburger-Will, S. Horn, *J. Mater. Sci.* **2018**, *53*, 4693.
- [49] a) H. Qiu, V. A. Du, M. A. Winnik, I. Manners, *J. Am. Chem. Soc.* **2013**, *135*, 17739; b) D. J. Lunn, O. E. C. Gould, G. R. Whittell, D. P. Armstrong, K. P. Mineart, M. A. Winnik, R. J. Spontak, P. G. Pringle, I. Manners, *Nat. Commun.* **2016**, *7*, 12371.

- [50] a) I. Osaka, R. D. McCullough, *Acc. Chem. Res.* **2008**, *41*, 1202; b) R. Zhang, B. Li, M. C. Iovu, M. Jeffries-EL, G. Sauvé, J. Cooper, S. Jia, S. Tristram-Nagle, D. M. Smilgies, D. N. Lambeth, R. D. McCullough, T. Kowalewski, *J. Am. Chem. Soc.* **2006**, *128*, 3480; c) M. C. Iovu, C. R. Craley, M. Jeffries-EL, A. B. Krankowski, R. Zhang, T. Kowalewski, R. D. McCullough, *Macromolecules* **2007**, *40*, 4733.
- [51] H. G. Elias, *Makromoleküle*, Vol. 1, Wiley-VCH GmbH Verlag, Weinheim, Germany **2005**.
- [52] a) D. Braun, H. Cherdron, M. Rehahn, H. Ritter, B. Voit, *Polymer Synthesis: Theory and Practice - Fundamentals, Methods, Experiments*, Springer-Verlag GmbH, Germany **2013**.
- [53] Deposition numbers CCDC 2358519 (1,4-bis(chlorodibutylsilyl)-2,5-*N,N,N',N'*-tetramethylphenylenediamine), 2358520 (1,4-dibromo-2,5-*N,N,N',N'*-tetrahexylphenylenediamine), 2358523 (1,4-bis(chlorodihexylsilyl)-2,5-*N,N,N',N'*-tetramethylphenylenediamine), 2358526 (**2b**), 2358527 (**2a**), 2358528 (**1a**), contain the supplementary crystallographic data for this paper. These data are provided free of charge by the joint Cambridge Crystallographic Data Centre and Fachinformationszentrum Karlsruhe Access Structures service.
- [54] N. Kuhn, T. Kratz, *Synthesis* **1993**, *1993*, 561.
- [55] T. Doornbos, J. Strating, *Org. Prep. Proced.* **1969**, *4*, 287.
- [56] G. R. Fulmer, A. J. M. Miller, N. H. Sherden, H. E. Gottlieb, A. Nudelman, B. M. Stoltz, J. E. Bercaw, K. I. Goldberg, *Organometallics* **2010**, *29*, 2176.
- [57] G. M. Sheldrick, *Acta Crystallogr. Sect. A* **2008**, *64*, 112.
- [58] G. M. Sheldrick, *Acta Crystallogr. Sect. A* **2015**, *71*, 3.
- [59] C. B. Hübschle, G. M. Sheldrick, B. Dittrich, *J. Appl. Crystallogr.* **2011**, *44*, 1281.
- [60] M. J. Frisch, G. W. Trucks, H. B. Schlegel, G. E. Scuseria, M. A. Robb, J. R. Cheeseman, G. Scalmani, V. Barone, B. Mennucci, G. A. Petersson, H. Nakatsuji, M. Caricato, X. Li, H. P. Hratchian, A. F. Izmaylov, J. Bloino, G. Zheng, J. L. Sonnenberg, M. Hada, M. Ehara, K. Toyota, R. Fukuda, J. Hasegawa, M. Ishida, T. Nakajima, Y. Honda, O. Kitao, H. Nakai, T. Vreven, J. J. A. Montgomery, J. E. Peralta, F. Ogliaro, M. Bearpark, J. J. Heyd, E. Brothers, K. N. Kudin, V. N. Staroverov, R. Kobayashi, J. Normand, K. Raghavachari, A. Rendell, J. C. Burant, S. S. Iyengar, J. Tomasi, M. Cossi, N. Rega, J. M. Millam, M. Klene, J. E. Knox, J. B. Cross, V. Bakken, C. Adamo, J. Jaramillo, R. Gomperts, R. E. Stratmann, O. Yazayev, A. J. Austin, R. Cammi, C. Pomelli, J. W. Ochterski, R. L. Martin, K. Morokuma, V. G. Zakrzewski, G. A. Voth, P. Salvador, J. J. Dannenberg, S. Dapprich, A. D. Daniels, O. Farkas, J. B. Foresman, J. V. Ortiz, J. Cioslowski, D. J. Fox, *Gaussian 16, Revision C.01*, Gaussian, Inc., Wallingford CT **2016**.
- [61] a) J. P. Perdew, *Phys. Rev. B* **1986**, *33*, 8822; b) A. D. Becke, *Phys. Rev. A* **1988**, *38*, 3098.
- [62] a) A. Schäfer, H. Horn, R. Ahlrichs, *J. Chem. Phys.* **1992**, *97*, 2571; b) A. Schäfer, C. Huber, R. Ahlrichs, *J. Chem. Phys.* **1994**, *100*, 5829; c) F. Weigend, R. Ahlrichs, *Phys. Chem. Chem. Phys.* **2005**, *7*, 3297; d) F. Weigend, *Phys. Chem. Chem. Phys.* **2006**, *8*, 1057.
- [63] a) S. Grimme, J. Antony, S. Ehrlich, H. Krieg, *J. Chem. Phys.* **2010**, *132*, 154104; b) S. Grimme, S. Ehrlich, L. Goerigk, *J. Comput. Chem.* **2011**, *32*, 1456.
- [64] a) A. E. Reed, R. B. Weinhold, F. Weinhold, *J. Chem. Phys.* **1985**, *83*, 735; b) A. E. Reed, L. A. Curtiss, F. Weinhold, *Chem. Rev.* **1988**, *88*, 899; c) E. D. Glendening, C. R. Landis, F. Weinhold, *J. Comput. Chem.* **2019**, *40*, 2234.
- [65] F. Neese, F. Wennmohs, U. Becker, C. Riplinger, *J. Chem. Phys.* **2020**, *152*, 224108.
- [66] a) J. P. Perdew, M. Ernzerhof, K. Burke, *J. Chem. Phys.* **1996**, *105*, 9982; b) C. Adamo, V. Barone, *J. Chem. Phys.* **1999**, *110*, 6158.
- [67] Chemcraft—graphical software for visualization of quantum chemistry computations. <https://www.chemcraftprog.com>.
- [68] J. Zhou, R. Tang, X. Wang, W. Zhang, X. Zhuang, F. Zhang, *J. Mater. Chem. C* **2016**, *4*, 1159.
- [69] C. C. Miller, *Proc. R. Soc. London, Ser. A* **1924**, *106*, 724.
- [70] J. H. Dymond, J. Robertson, J. D. Isdale, *Int. J. Thermophys.* **1981**, *2*, 223.
- [71] C. S. Johnson, *Prog. Nucl. Magn. Reson. Spectrosc.* **1999**, *34*, 203.
- [72] S. Berger, S. Braun, *200 and More NMR Experiments*, Wiley-VCH Verlag GmbH & Co. KGaA, Weinheim **2004**.
- [73] E. O. Stejskal, J. E. Tanner, *J. Chem. Phys.* **1965**, *42*, 288.
- [74] M. Nilsson, M. A. Connell, A. L. Davis, G. A. Morris, *Anal. Chem.* **2006**, *78*, 3040.
- [75] P.-J. Voorter, A. McKay, J. Dai, O. Paravagna, N. R. Cameron, T. Junkers, *Angew. Chem.* **2022**, *134*, e202114536; *Angew. Chem. Int. Ed.* **2022**, *61*, e202114536.
- [76] P. J. Mohr, B. N. Taylor, D. B. Newell, *Rev. Mod. Phys.* **2012**, *84*, 1527.

Manuscript received: August 14, 2024

Accepted manuscript online: October 23, 2024

Version of record online: November 16, 2024